

Journal Pre-proofs

A combined experimental and theoretical study on an ionic cobalt(III/II) complex with a Schiff base ligand

Kousik Ghosh, Tamal Dutta, Michael G.B. Drew, Antonio Frontera, Shouvik Chattopadhyay

PII: S0277-5387(20)30089-9
DOI: <https://doi.org/10.1016/j.poly.2020.114432>
Reference: POLY 114432

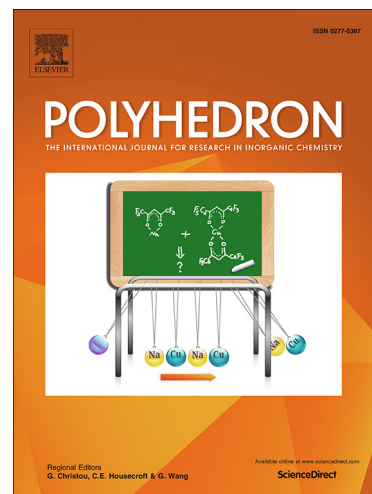
To appear in: *Polyhedron*

Received Date: 17 December 2019
Revised Date: 27 January 2020
Accepted Date: 4 February 2020

Please cite this article as: K. Ghosh, T. Dutta, M.G.B. Drew, A. Frontera, S. Chattopadhyay, A combined experimental and theoretical study on an ionic cobalt(III/II) complex with a Schiff base ligand, *Polyhedron* (2020), doi: <https://doi.org/10.1016/j.poly.2020.114432>

This is a PDF file of an article that has undergone enhancements after acceptance, such as the addition of a cover page and metadata, and formatting for readability, but it is not yet the definitive version of record. This version will undergo additional copyediting, typesetting and review before it is published in its final form, but we are providing this version to give early visibility of the article. Please note that, during the production process, errors may be discovered which could affect the content, and all legal disclaimers that apply to the journal pertain.

© 2020 Elsevier Ltd. All rights reserved.



A combined experimental and theoretical study on an ionic cobalt(III/II) complex with a Schiff base ligand

Kousik Ghosh^a, Tamal Dutta^a, Michael G.B. Drew^b, Antonio Frontera^{c,*} and Shouvik Chattopadhyay^{a,*}

^aDepartment of Chemistry, Inorganic Section, Jadavpur University, Kolkata - 700032, India. Tel: +913324572147 e-mail: shouvik.chem@gmail.com.

^bSchool of Chemistry, The University of Reading, P.O. Box 224, Whiteknights, Reading RG6 6AD, UK.

^cDepartamento de Química, Universitat de les Illes Balears, Crta. de Valldemossa km 7.5, 07122 Palma (Balears), Spain.

Abstract

An ionic cobalt(III/II) complex, $[\text{Co}^{\text{III}}(\text{L})_2][\text{Co}^{\text{II}}(\text{NCS})_3(\text{H}_2\text{O})]$, where $\text{H}_2\text{L} = 2-((3\text{-aminopropylimino)methyl})\text{-6-methoxyphenol}$, has been synthesized and characterized by several analytical techniques, including single crystal X-ray diffraction analysis. The energetic features of the solid state non-covalent interactions involved in the titled ionic coordination complex have been studied by means of DFT computations, which indicate that a combination of strong $\text{CH}_3 \cdots \pi$ and H-bonding interactions is the main reason behind the stabilization of this complex.

Keywords: Ionic cobalt(III/II) complex; Crystal structure; DFT calculations

1. Introduction

Various di-/tri-/poly-nuclear transition metal complexes have attracted interest from inorganic chemists owing to the diversity of their structural features and potential applications in the field of condensed physics and material chemistry [1-4]. Another inherent potential of these complexes is their efficacy in modelling the multi-metal active sites of biomolecules [5-7]. Dinuclear cobalt complexes may function as mimics of active biosites, such as in methionine amino peptidase [8,9], and can show DNA cleavage activity [10]. Alternatively, Schiff base ligands themselves have been widely used in coordination chemistry due to their facile syntheses, easily tunable steric and electronic properties, and their applications in different branches of science [11-15]. Transition metal complexes of Schiff base ligands are important stereochemical models in main group and transition metal coordination chemistry [11-16]. These complexes have wide applications, including bioinorganic chemistry, material science and magnetism, bio-relevant catalytic activities, separation and encapsulation, hydrometallurgy, metal clusters, transport and activation of small molecules etc [16-24].

Herein, we report a new ionic cobalt(III/II) complex, $[\text{Co}^{\text{III}}(\text{L})_2][\text{Co}^{\text{II}}(\text{NCS})_3(\text{H}_2\text{O})]$, derived from a mono-condensed Schiff base and thiocyanate co-ligands. Single crystal X-ray crystallography analysis confirms that the complex is an ionic cobalt(III/II) complex with one tetracoordinated cobalt(II) centre. To find out the reason behind such a unique structure in the solid state, complete DFT calculations have been performed, which confirmed that a combination of $\text{CH}_3 \cdots \pi$ and hydrogen bonding interactions plays a vital role in the stabilization of the titled ionic complex.

2. Material and methods

2.1. Starting materials and solvents

The starting materials and solvents used in this work were purchased from Sigma-Aldrich, India (now Merck, India) and were of reagent grade. They were used as received, without any further purification. The entire syntheses and manipulations were carried out under aerobic conditions.

2.2. Preparation of $[Co^{III}(L)_2][Co^{II}(NCS)_3(H_2O)]$

0.10 mL (~1 mmol) of 1,3-diaminopropane was mixed with 304 mg (~2 mmol) of 3-methoxysalicylaldehyde in 25 mL of a 2:1 (v/v) methanol-acetonitrile mixture. The resulting mixture was refluxed for c.a. 1.5 h and allowed to cool. A methanol solution (10 ml) of cobalt(II) acetate tetrahydrate (500 mg, ~2 mmol) was then directly added to this yellow coloured solution of the Schiff base ligand, followed by the addition of a methanol solution (10 mL) of sodium thiocyanate (162 mg, ~2 mmol) with constant stirring. The stirring was continued for an additional 1.5 h and then the reaction mixture was filtered into a beaker. The filtrate was allowed to stand overnight until X-ray quality single crystals were viewed at the bottom of the beaker. The crystals were dried in a desiccator containing anhydrous $CaCl_2$ and then characterized by single crystal X-ray diffraction, elemental analysis and spectroscopic methods.

Yield: 685 mg (~54%); based on cobalt(III). Anal. Calc. for $C_{48}H_{64}Co_3N_{11}O_{12}S_3$ (FW = 1260.10): C, 45.75; H, 5.12; N, 12.23%. Found: C, 45.9; H, 5.0; N, 12.3%. FT-IR (KBr, cm^{-1}): 3245-3214 (ν_{N-H}), 2930-2910 (ν_{C-H}), 2064 (ν_{NCS}), 1624 ($\nu_{C=N}$), 1439 ($\nu_{C=C}$). UV-Vis λ_{max} (nm), $[\epsilon_{max} (dm^3 mol^{-1} cm^{-1})]$ (DMF): 540 (4.32×10^2), 396 (6.04×10^4), 273 (7.24×10^4). Crystal data and refinement details: Crystal System = Triclinic, Temperature (K) = 150(2), D_{calc} (g/cm^3) = 1.360, Space group = $P\bar{1}$, a (Å) = 11.3567(7), b (Å) = 11.7058(8), c (Å) = 13.3789(8), α (°) =

66.228(6), β ($^\circ$) = 89.455(5), γ ($^\circ$) = 72.416(6), μ (mm^{-1}) = 0.963, $F(000)$ = 654, Total Reflections = 7473, Unique Reflections = 5314, Observed data [$I > 2 \sigma(I)$] = 4819, No of parameters = 416, $R(\text{int})$ = 0.026, R_1 , $wR_2(\text{all data})$ = 0.1146, 0.2892, R_1 , $wR_2([I > 2 \sigma(I)]$ = 0.1081, 0.2861, Residual Electron Density ($e \text{ \AA}^{-3}$) = 0.765, -0.701.

2.3. Details of instrumentation

Single crystal X-ray diffraction was performed using an Oxford Diffraction X Calibur diffractometer equipped with graphite-monochromated molybdenum K_α radiation ($\lambda = 0.71073 \text{ \AA}$). Additional instrumentation details have been given in the Supplementary Information section.

2.4. Hirshfeld surface analysis

Crystal Explorer [25] was used to calculate the Hirshfeld surfaces [26,27] and associated 2D fingerprint plots [28-30] of the complex. Further details can be found in the Supplementary Information section.

2.5. Theoretical methods

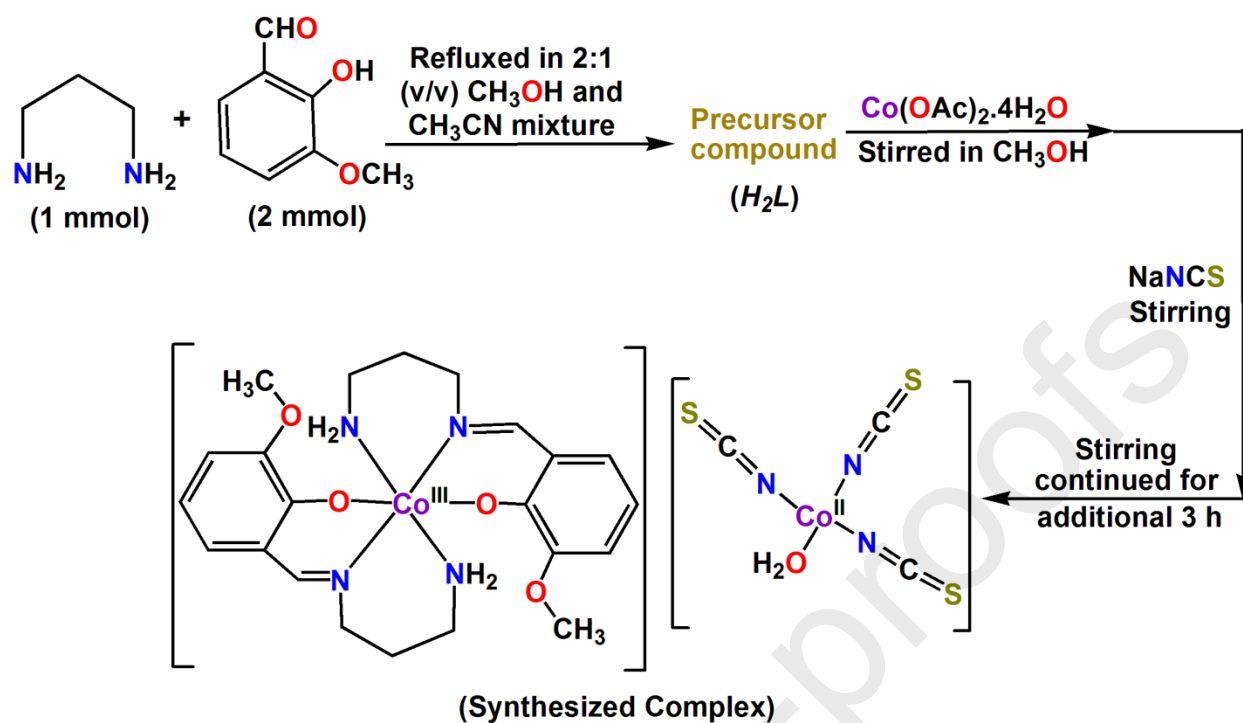
The energies of the complexes included in this study were computed at the B3LYP-D/def2-SVP level of theory using the crystallographic coordinates. For the calculations we have used the GAUSSIAN-09 program [31]. The same level of theory was used for the molecular electrostatic potential (MEP) surface calculations. We have also used Grimme's dispersion [32] correction since it is adequate for the evaluation of non-covalent interactions. The basis set superposition error for the calculation of interaction energies has been corrected using the counterpoise method [33]. The NCI plot [34] isosurfaces have been used to characterize non-

covalent interactions. They correspond to both favorable and unfavorable interactions, as differentiated by the sign of the second density Hessian Eigen value and defined by the isosurface color. The color scheme is a red-yellow-green-blue scale, with red for ρ^+_{cut} (repulsive) and blue for ρ^-_{cut} (attractive). The Gaussian-09 B3LYP-D/def2-SVP wavefunction has been used to generate the NCI plot.

3. Results and discussion

3.1. Synthesis of the complex

In present work, a new ionic cobalt(III/II) complex was synthesized. The formation of this complex can be rationalized in light of the one pot synthesis method. The Schiff base ligand was synthesized using a previously reported synthetic route [35-38]. The Schiff base ligand (HL), on reaction with cobalt(II) acetate tetrahydrate and sodium thiocyanate, resulted in an ionic complex, $[\text{Co}^{\text{III}}(\text{L})_2][\text{Co}^{\text{II}}(\text{NCS})_3(\text{H}_2\text{O})]$. It is obvious that initially a tetradentate Schiff base was formed, which partially hydrolyzed under the reaction conditions to produce a tridentate Schiff base ligand (HL). As the solvents were not dried, a lot of water may be present in the methanol. This increased concentration of water might be responsible for initiating the hydrolysis. The synthetic route to the complex is shown in Scheme 1.



Scheme 1: Synthetic route to the complex.

3.2 Crystal structure description of the complex

Single crystal X-ray structure determination reveals that the synthesized complex consists of a discrete dinuclear unit, $[\text{Co}^{\text{III}}(\text{L})_2][\text{Co}^{\text{II}}(\text{NCS})_3(\text{H}_2\text{O})]$. The complex crystallizes in the triclinic system with the $P\bar{1}$ space group. A perspective view of the ionic coordination complex along with the metal centre coordinated atom numbering scheme is illustrated in Figure 1. Relevant bond angles are summarized in Table 1. The titled complex consists of one cationic complex part, $[\text{Co}^{\text{III}}(\text{L})_2]^+$, and one anionic complex part, $[\text{Co}^{\text{II}}(\text{NCS})_3(\text{H}_2\text{O})]^-$. In the cationic part of the complex, there are two independent mononuclear subunits (A and B) with equivalent geometries. Subunit B has a very similar molecular structure; the structural details and relevant figures are provided in the Supplementary Information (Figure S1).

In subunit A of the cationic part, the cobalt(III) centre, Co(1), exhibits a slightly distorted octahedral coordination geometry, with two imine nitrogen atoms, N(19A) and N(19A)^a, two amine nitrogen atoms, N(23A) and N(23A)^a, and two phenoxo oxygen atoms, O(11A) and O(11A)^a, from two deprotonated Schiff base ligands (L⁻) to complete its octahedral geometry. The saturated six membered chelate rings, Co(1)-N(19A)-C(20A)-C(21A)-C(22A)-N(23A) and Co(1)-N(19A)^a-C(20A)^a-C(21A)^a-C(22A)^a-N(23A)^a, present chair conformations with puckering parameters [39,40] $Q = 0.647(8) \text{ \AA}$, $\theta = 11.3(7)^\circ$, $\phi = 27(4)^\circ$ and $Q = 0.647(8) \text{ \AA}$, $\theta = 168.7(7)^\circ$, $\phi = 207(4)^\circ$, respectively (Symmetry transformation; ^a = -x,-y,-z). The Co(III)-N_{imine} distances are shorter than the Co(III)-N_{amine} ones, due to the different hybridization of the nitrogen atoms. This is a common phenomenon observed in many other cobalt(III) Schiff base complexes [35,37].

In the anionic complex part, the cobalt(II) ion exhibits a slightly distorted tetrahedral coordination sphere, in which the cobalt(II) ion is coordinated by three thiocyanate nitrogen atoms, N(1), N(2) and N(3), and a water oxygen atom, O(1W). Although tetra-coordinated cobalt(II) ions are not routinely noticed, in many previously published papers the presence of tetra-coordinated cobalt(II) complexes are observed [41-45]. The bond angles (given in Table 1) highly deviate from a perfect tetrahedral geometry ($\sim 109.5^\circ$), which confirms the distorted tetrahedral geometry around the central cobalt(II) ion. The N-C-S angles in the terminal thiocyanate coligands are 180(3) for N(1)-C(1)-S(1), 172(2) for N(2)-C(2)-S(2) and 179(3) for N(3)-C(3)-S(3), which indicate more or less linear arrangements.

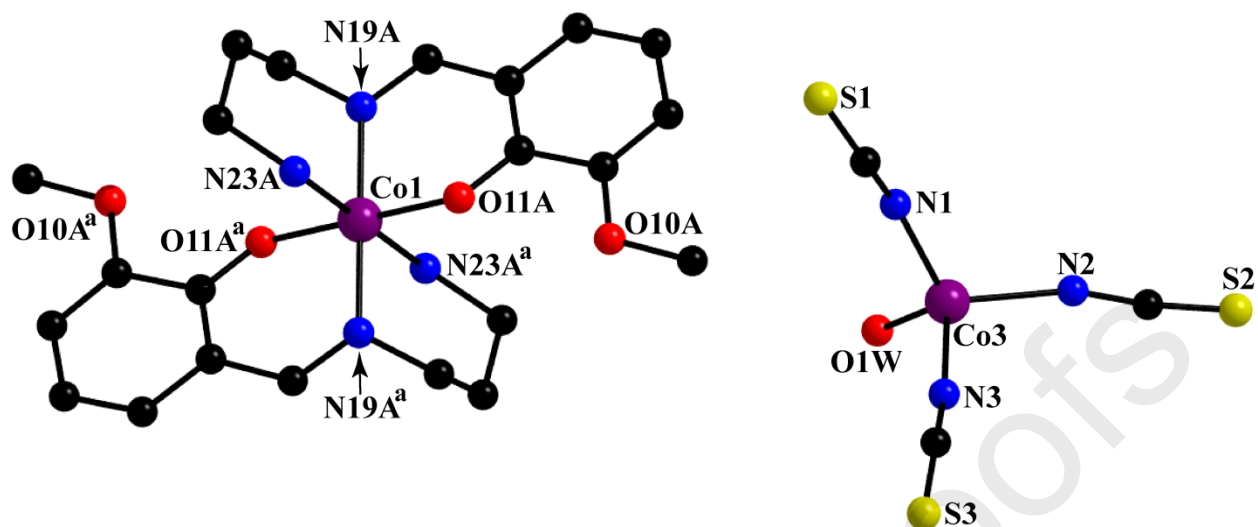


Figure 1: Molecular structure of the titled complex with a selective atom numbering scheme.

Only the major component of the disorder has been shown. Hydrogen atoms have been omitted

for clarity. Bond lengths in Å: Co(1)-O(11A) = 1.907(6), Co(1)-N(19A) = 1.931(7), Co(1)-N(23A) = 1.979(8), Co(1)-O(11A)^a = 1.907(6), Co(1)-N(19A)^a = 1.931(7), Co(1)-N(23A)^a = 1.979(8), Co(3)-N(3) = 1.95(2), Co(3)-N(1) = 1.94(2), Co(3)-N(2) = 2.07(2), Co(3)-O(1W) = 2.03(2) (Symmetry transformation; ^a = -x,-y,-z).

3.3 Theoretical calculations

The theoretical study is devoted to analyse the energy associated with the combination of $\text{CH}_3 \cdots \pi$ and hydrogen bonding interactions observed in the solid state of the titled complex and to characterize them using MEP and NCI plot computational tools.

First, we computed the MEP surface of the $[\text{Co}^{\text{III}}(\text{L})_2]^+$ complex cation that is depicted in Figure 2. The most negative MEP value is located between the oxygen atoms of the Schiff base ligands (-50 kcal/mol). The most positive value is located at the hydrogen atoms of the methoxide group (+20 kcal/mol), that is unexpectedly more positive than the values of the MEP

at the hydrogen atoms of the coordinated amino group. Finally, the MEP value over the aromatic ring is significantly negative, thus well suited for interacting with electron deficient regions.

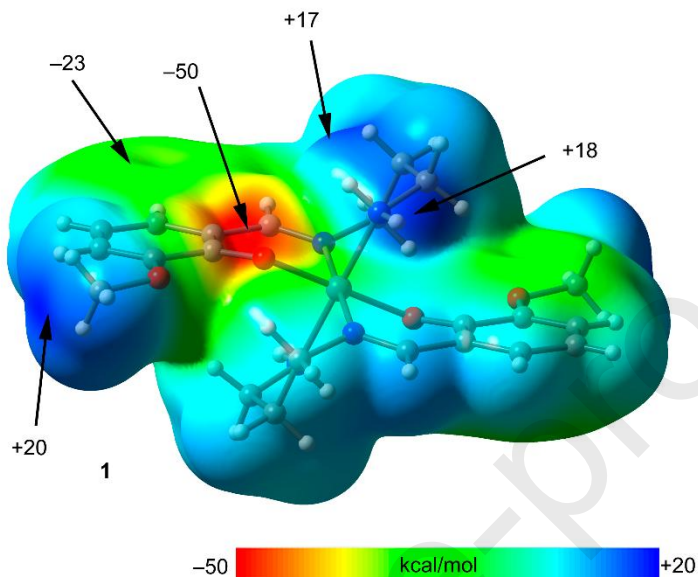


Figure 2: MEP surface (isodensity = 0.001 a.u.) of the cationic part of the synthesized complex, $[\text{Co}^{\text{III}}(\text{L})_2]^+$. The values at selected points of the surface are indicated. Negative and positive values are highlighted in red and blue colours, respectively.

In Figure 3(a) we show a partial view of the X-ray structure of the titled complex, where the $[\text{Co}^{\text{III}}(\text{L})_2]^+$ cationic moieties form an infinite 1D tape in the solid state. Moreover, the tapes are sandwiched by the $[\text{Co}^{\text{II}}(\text{NCS})_3(\text{H}_2\text{O})]^-$ anionic counterparts. We have first analyzed one dimer of $[\text{Co}^{\text{III}}(\text{L})_2]^+$ extracted from the infinite 1D chain {Figure 3(b)}. It can be observed that its formation is governed by a combination of bifurcated hydrogen bonds between the N-H group and the oxygen atoms of the ligand, and quite short $\text{CH}_3 \cdots \pi$ interactions. The formation of the latter interactions agrees well with the MEP surface analysis, since the most positive MEP value is located at the methyl group. Moreover, the MEP over the aromatic ring is large and negative, likely due to the anionic nature of the ligand. As a consequence, the dimerization energy is large

($\Delta E_1 = -41.0$ kcal/mol) due to the formation of two bifurcated hydrogen bonds and the electrostatically enhanced $\text{CH}_3 \cdots \pi$ interactions. In this dimer, there are two N-H groups {double arrow in Figure 3(b)} that converge to the same spatial region and thus are adequate to interact with the electron rich thiocyanate ligand of the $[\text{Co}^{\text{II}}(\text{NCS})_3(\text{H}_2\text{O})]^-$ anionic counterpart. We have also evaluated the interaction energy of the complex between the $[\text{Co}^{\text{III}}(\text{L})_2]^+$ dimer and $[\text{Co}^{\text{II}}(\text{NCS})_3(\text{H}_2\text{O})]^-$, which is also very large, $\Delta E_2 = -20.3$ kcal/mol.

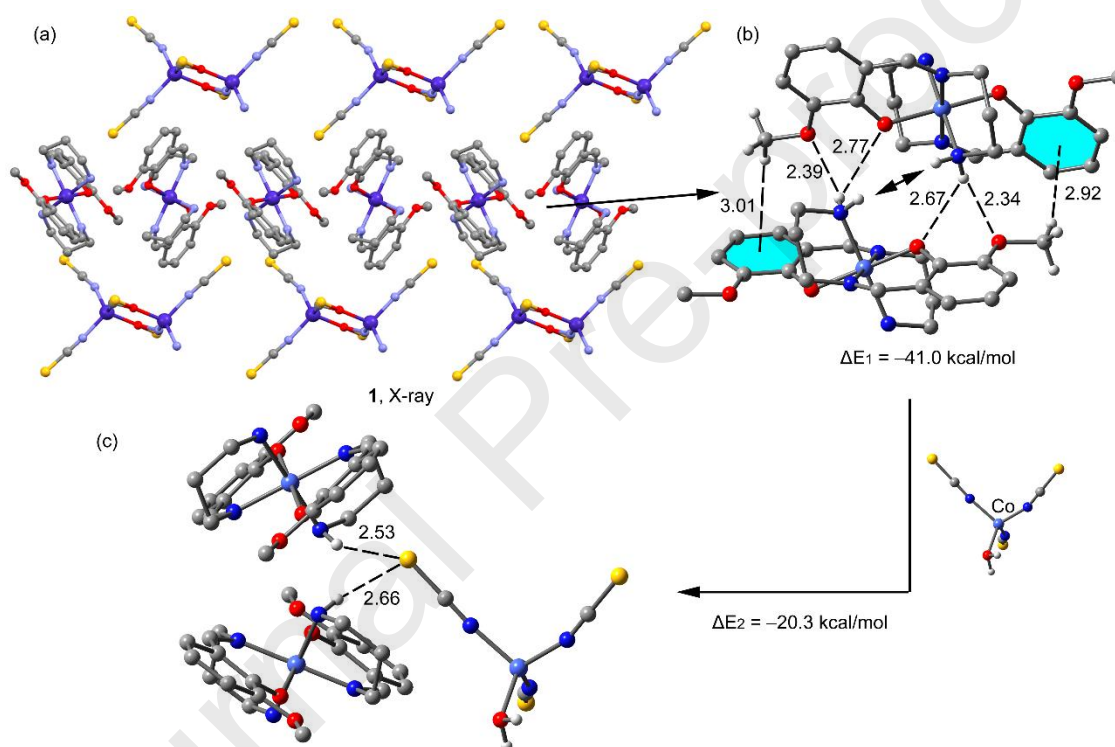


Figure 3: (a) Partial view of the X-ray structure of the titled complex. Hydrogen atoms are omitted for clarity. (b) Theoretical model used to evaluate the non-covalent interactions (distances are indicated in Å). Only the relevant hydrogen atoms are shown. (c) Theoretical model used to evaluate the interaction of the dimer with the $[\text{Co}^{\text{II}}(\text{NCS})_3(\text{H}_2\text{O})]^-$ anionic moiety.

We have also computed the “non-covalent Interaction plot” (NCI plot) index in order to characterize the non-covalent interactions in the dimer of the titled complex. The NCI plot is a

visualization index that can identify and characterize non-covalent interactions easily and efficiently since it clearly shows which molecular regions interact. The colour code for the isosurfaces is the red-yellow-green-blue scale, with red being repulsive and blue being attractive. Yellow and green surfaces correspond to weakly repulsive and weakly attractive interactions, respectively. The representation for the dimer of the titled complex is shown in Figure 4. The presence of green isosurfaces located between the $-\text{CH}_3$ groups and the aromatic rings is observed, thus confirming the $\text{CH}_3 \cdots \pi$ interactions. The NCI plot shows the existence of several smaller isosurfaces that characterize the bifurcated $\text{N-H} \cdots \text{O}$ hydrogen bonds and also reveals the existence of ancillary $\text{C-H} \cdots \text{O}$ interactions that also contribute to the stabilization of the assembly. Finally, this analysis also reveals the existence of long range van der Waals interactions due to the approximation of the bulk of both molecules.

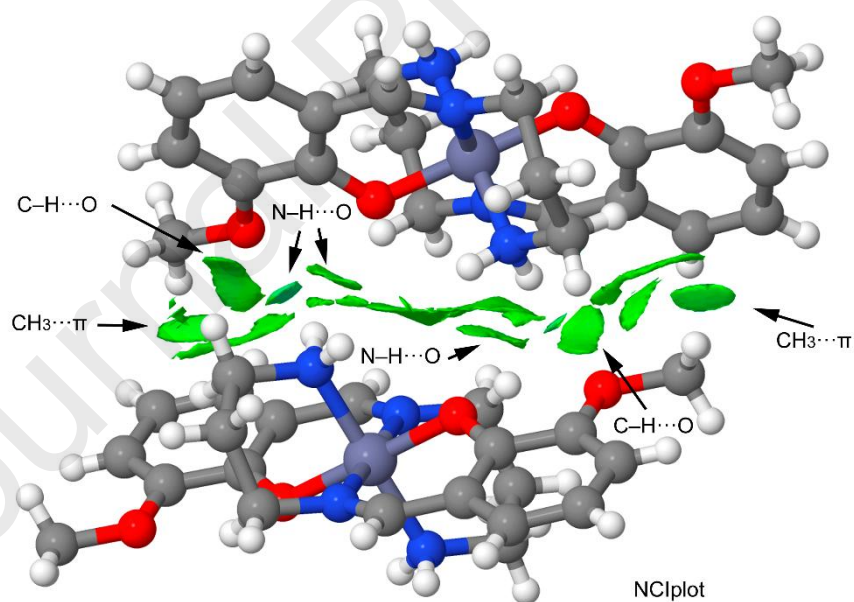


Figure 4: NCI surface of the assembly in the synthesized complex. The gradient cut-off is $s = 0.35$ au, and the color scale is $-0.04 < \rho < 0.04$ au. Only intermolecular interactions are depicted for clarity.

3.4. Hirshfeld surface analysis

The solid state crystal structure of any complex can be determined by an amalgamation of a number of important intermolecular and intramolecular interactions, and therefore all these interactions should be considered. Hirshfeld surface analysis helps us to visualize and investigate these important supramolecular interactions. Visualization and investigation of these major interactions using the Hirshfeld surface based technique symbolizes a vital progress in enabling supramolecular chemists and crystal engineers to gain insight into crystal packing. The Hirshfeld surfaces of the titled complex were mapped over none, d_i , d_e , d_{norm} , shape index and curvedness (Figure 5). The surfaces are shown as transparent so that the molecular moieties around which the Hirshfeld surfaces are calculated could be easily picturize. The predominant interactions in the complex are $\text{H}\cdots\text{H}$, $\text{C}\cdots\text{H}/\text{H}\cdots\text{C}$, $\text{O}\cdots\text{H}/\text{H}\cdots\text{O}$, $\text{N}\cdots\text{H}/\text{H}\cdots\text{N}$ and $\text{S}\cdots\text{H}/\text{H}\cdots\text{S}$. Bright red spots on the d_{norm} surface (Figure 5) indicate that these interactions are predominant. Additionally, 2D fingerprint plots (Figure 6) exemplify the various inter-molecular interaction patterns associated with the complex and their relative contributions are given on the percentage scale. In the 2D fingerprint plots, the inter-molecular interactions become visible as distinct spikes. Complementary regions are visible in the two dimensional fingerprint plots where one molecule acts as a donor ($d_e > d_i$) and the other as an acceptor ($d_e < d_i$). The fingerprint plots can also be decomposed to highlight preferred atom pair close contacts. This decomposition enables the separation of contributions from different interaction types, which overlap in the full fingerprint [46].

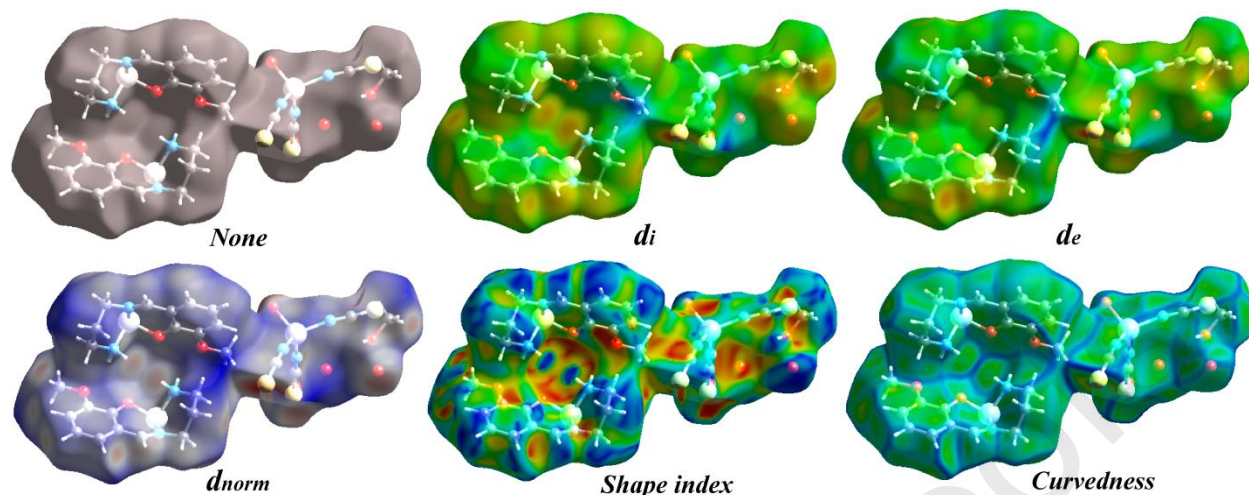


Figure 5: Hirshfeld surfaces of the synthesized complex mapped over none, d_i , d_e , d_{norm} , shape index and curvedness.

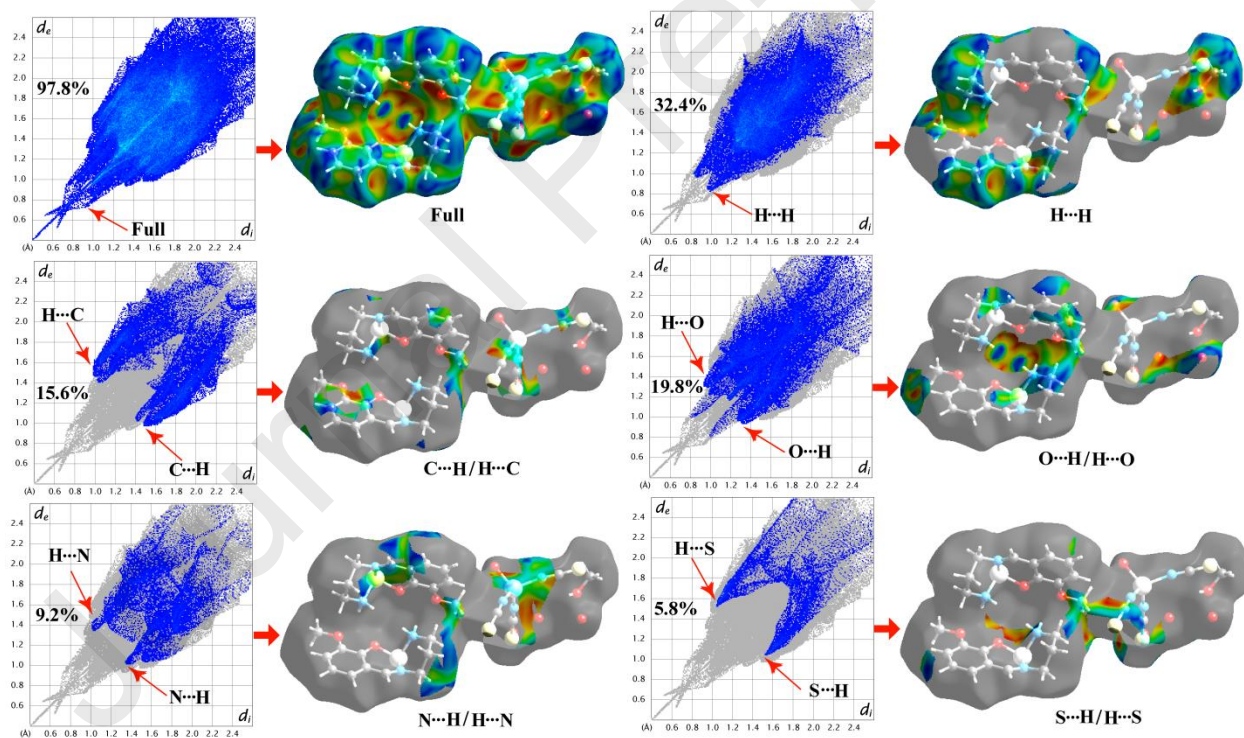


Figure 6: Two dimensional fingerprint plots of the complex: Full and resolved into H...H, C...H / H...C, O...H / H...O, N...H / H...N and S...H / H...S contacts showing the percentages of contacts contributing to the total Hirshfeld surface area of the complex. Surfaces in the right

hand columns highlight the relevant surface patches associated with the specific contacts in the total Hirshfeld surface area of the complex.

3.5. IR and electronic spectroscopy

The IR and electronic spectra of the synthesized complex are in good agreement with its crystal structure. Some of the exceptionally informative infrared and electronic absorption peaks which assist in the structural characterization of the complex are gathered in the Experimental section. Moderately strong bands in the range 3245-3214 cm^{-1} (due to N-H stretching) confirm the presence of a free amine group in the titled complex [47-49]. The band corresponding to the azomethine (C=N) group is distinct and occurs at 1624 cm^{-1} [35,37,50]. The lowering of the positions of these bands indicates their coordination with the metal centres. The appearance of a strong band at 2064 cm^{-1} indicates the presence of an N-coordinated thiocyanate group in the complex [35,37]. The bands in the range 2930-29100 cm^{-1} due to alkyl C-H stretching vibrations are noted [35,37]. The IR spectrum of the synthesized complex is given in Figure S2 (Supplementary Information).

The UV-Vis absorption spectrum of the complex in DMF shows a low energy absorption band at 540 nm, attributable to a transition in the visible region of a low-spin cobalt(III) ion in an octahedral geometry, obscuring the transitions of the divalent metal ion [47,51]. Bands arising from d-d transitions of the cobalt(II) ion are Laporte forbidden and are assumed to be too weak to be visible. In addition to these low-energy d-d transition bands, an absorption band at 396 nm was observed in the electronic spectrum of the complex, which may be assigned as a ligand-to-metal charge transfer transition [51,52]. Moreover, a high energy absorption band at 273 nm was observed in the electronic spectrum of the complex, which may be recognized as intra-ligand π -

$\pi^*/n-\pi^*$ transitions [51,52]. The electronic spectrum of the synthesized complex is given in Figure S3 (Supplementary Information).

4. Concluding remarks

In conclusion, we have discussed the synthetic stratagem and structural characterization of a new ionic cobalt(III/II) complex. The structure of the complex was confirmed by the single crystal X-ray diffraction technique. The complex exhibits a combination of strong $\text{CH}_3 \cdots \pi$ and H-bonding interactions in the solid state that have been rationalized using MEP surface analysis. The energies associated with the interactions have been computed using DFT calculations and further corroborated with the NCI plot index computational tool.

Acknowledgements

K.G. expresses his gratitude to UGC, India for awarding a Senior Research Fellowship.

Appendix A. Supplementary data

CCDC 1970250 contains the supplementary crystallographic data of the titled complex. These data can be obtained free of charge via <http://www.ccdc.cam.ac.uk/conts/retrieving.html>, or from the Cambridge Crystallographic Data Centre, 12 Union Road, Cambridge CB2 1EZ, UK; fax: (+44) 1223-336-033; e-mail: deposit@ccdc.cam.ac.uk.

References:

- [1] S. Roy, A. Dey, P. P. Ray, J. Ortega-Castro, A. Frontera, S. Chattopadhyay, *Chem. Commun.* 51 (2015) 12974-12976.
- [2] S. V. Krivovichev, *Eur. J. Inorg. Chem.* (2010) 2594-2603.

- [3] M. Yuan, Y. Li, E. Wang, C. Tian, L. Wang, C. Hu, N. Hu, H. Jia, *Inorg. Chem.* 42 (2003) 3670-3676.
- [4] K. Ghosh, S. Sil, P. P. Ray, J. Ortega-Castro, A. Frontera, S. Chattopadhyay, *RSC Adv.* 9 (2019) 34710-34719.
- [5] T. Basak, M. G. B. Drew, S. Chattopadhyay, *Inorg. Chem. Commun.* 98 (2018) 92-98.
- [6] T. Liu, J. Tian, L. Cui, Q. Liu, L. Wu, X. Zhang, *Colloids Surf., B* 178 (2019) 197-145.
- [7] R. E.H.M.B. Osório, A. Neves, T. P. Camargo, S. L. Mireski, A. J. Bortoluzzi, E. E. Castellano, W. Haase, Z. Tomkowicz, *Inorg. Chim. Acta* 435 (2015) 153-158.
- [8] L. J. Daumann, P. Comba, J. A. Larrabee, G. Schenk, R. Stranger, G. Cavigliasso, L. R. Gahan, *Inorg. Chem.* 52 (2013) 2029-2043.
- [9] Z. A. K. Khattak, H. A. Younus, N. Ahmad, H. Ullah, S. Suleman, M. S. Hossain, M. Elkadi, F. Verpoort, *Chem. Commun.* 55 (2019) 8274-8277.
- [10] R. Eshkourfu, B. Čobeljić, M. Vujčić, I. Turel, A. Pevec, K. Sepčić, M. Zec, S. Radulović, T. Srdić-Radić, D. Mitić, K. Andjelković, D. Sladić, *J. Inorg. Biochem.* 105 (2011) 1196-1203.
- [11] S. Chandra, S. Sangeetika, *Spectrochim. Acta A* 60 (2004) 147-153.
- [12] B. J. Hathaway, D. E. Billing, *Coord. Chem. Rev.* 5 (1970) 143-207.
- [13] C. -M. Che, J. -S. Huang, *Coord. Chem. Rev.* 242 (2003) 97-113.
- [14] M. Kojima, H. Taguchi, M. Tsuchimoto, K. Nakajima, *Coord. Chem. Rev.* 237 (2003) 183-196.

- [15] M. Calligaris, L. Randaccio, in: G. Wilkinson (Ed.), *Comprehensive Coordination Chemistry*, Pergamon Press, Oxford, 1987.
- [16] B. De Clercq, F. Verpoort, *Macromolecules* 35 (2002) 8943-8947.
- [17] X. Liu, J. -R. Hamon, *Coord. Chem. Rev.* 389 (2019) 94-118.
- [18] B. De Clercq, F. Lefebvre, F. Verpoort, *Appl. Catal. A* 247 (2003) 345-364.
- [19] S. L. Lambert, C. L. Spiro, R. R. Gagne, D. N. Hendrickson, *Inorg. Chem.* 21 (1982) 68-72.
- [20] S. Brooker, *Coord. Chem. Rev.* 222 (2001) 33-56.
- [21] É. N. Oiyé, M. F. M. Ribeiro, J. M. T. Katayama, M. C. Tadini, M. A. Balbino, I. C. Eleotério, J. Magalhães, A. S. Castro, R. S. M. Silva, J. W. da Cruz Júnior, E. R. Dockal, M. F. de Oliveira, *Crit. Rev. Anal. Chem.* 49 (2019) 488-509.
- [22] P. A. Vigato, S. Tamburini, *Coord. Chem. Rev.* 248 (2004) 1717-2128.
- [23] A. De, H. P. Ray, P. Jain, H. Kaur, N. Singh, *J. Mol. Struct.* 1199 (2020) 126901.
- [24] K. Ghosh, S. Pattanayak, A. Chakravorty, *Organometallics* 17 (1998) 1956-1960.
- [25] S. K. Wolff, D. J. Grimwood, J. J. McKinnon, D. Jayatilaka, M. A. Spackman, *Crystal Explorer 2.0*; University of Western Australia: Perth, Australia, (2007).
<http://hirshfeldsurfacenet.blogspot.com/>.
- [26] M. A. Spackman, D. Jayatilaka, *CrystEngComm.* 11 (2009) 19-32.
- [27] H. F. Clausen, M. S. Chevallier, M. A. Spackman, B. B. Iversen, *New J. Chem.* 34 (2010) 193-199.

- [28] A. L. Rohl, M. Moret, W. Kaminsky, K. Claborn, J. J. McKinnon, B. Kahr, *Cryst. Growth Des.* 8 (2008) 4517-4525.
- [29] A. Parkin, G. Barr, W. Dong, C. J. Gilmore, D. Jayatilaka, J. J. McKinnon, M. A. Spackman, C. C. Wilson, *CrystEngComm.* 9 (2007) 648-652.
- [30] M. A. Spackman, J. J. McKinnon, *CrystEngComm.* 4 (2002) 378-392.
- [31] M. J. Frisch, G. W. Trucks, H. B. Schlegel, G. E. Scuseria, M. A. Robb, J. R. Cheeseman, G. Scalmani, V. Barone, B. Mennucci, G. A. Petersson, H. Nakatsuji, M. Caricato, X. Li, H. P. Hratchian, A. F. Izmaylov, J. Bloino, G. Zheng, J. L. Sonnenberg, M. Hada, M. Ehara, K. Toyota, R. Fukuda, J. Hasegawa, M. Ishida, T. Nakajima, Y. Honda, O. Kitao, H. Nakai, T. Vreven, J. A. Montgomery, Jr., J. E. Peralta, F. Ogliaro, M. Bearpark, J. J. Heyd, E. Brothers, K. N. Kudin, V. N. Staroverov, R. Kobayashi, J. Normand, K. Raghavachari, A. Rendell, J. C. Burant, S. S. Iyengar, J. Tomasi, M. Cossi, N. Rega, J. M. Millam, M. Klene, J. E. Knox, J. B. Cross, V. Bakken, C. Adamo, J. Jaramillo, R. Gomperts, R. E. Stratmann, O. Yazyev, A. J. Austin, R. Cammi, C. Pomelli, J. W. Ochterski, R. L. Martin, K. Morokuma, V. G. Zakrzewski, G. A. Voth, P. Salvador, J. J. Dannenberg, S. Dapprich, A. D. Daniels, Ö. Farkas, J. B. Foresman, J. V. Ortiz, J. Cioslowski, D. J. Fox, *Gaussian 09* (Gaussian, Inc., Wallingford CT, 2009).
- [32] S. Grimme, J. Antony, S. Ehrlich, H. Krieg, *J. Chem. Phys.* 132 (2010) 154104.
- [33] S. F. Boys, F. Bernardi, *Mol. Phys.* 19 (1970) 553-566.
- [34] J. Contreras-García, E. R. Johnson, S. Keinan, R. Chaudret, J. -P. Piquemal, D. N. Beratan, W. Yang, *J. Chem. Theory Comput.* 7 (2011) 625-632.

- [35] K. Ghosh, S. Roy, A. Ghosh, A. Banerjee, A. Bauzá, A. Frontera, S. Chattopadhyay, *Polyhedron* 112 (2016) 6-17.
- [36] T. Basak, A. Bhattacharyya, M. Das, K. Harms, A. Bauzá, A. Frontera, S. Chattopadhyay, *ChemistrySelect* 2 (2017) 6286-6295.
- [37] K. Ghosh, K. Harms, S. Chattopadhyay, *Polyhedron* 123 (2017) 162-175.
- [38] S. Roy, A. Bhattacharyya, S. Herrero, R. González-Prieto, A. Frontera, S. Chattopadhyay, *ChemistrySelect* 2 (2017) 6535-6543.
- [39] D. Cremer, J. A. Pople, *J. Am. Chem. Soc.* 97 (1975) 1354-1358.
- [40] A. D. Hill, P. J. Reilly, *J. Chem. Inf. Model.* 47 (2007) 1031-1035.
- [41] J. M. Zadrozny, J. Telser, J. R. Long, *Polyhedron* 64 (2013) 209-217.
- [42] C. Bianchini, G. Mantovani, A. Meli, F. Migliacci, *Organometallics* 22 (2003) 2545-2547.
- [43] A. Buchholz, A. O. Eseola, W. Plass, *C. R. Chimie* 15 (2012) 929-936.
- [44] K. Fukui, H. O. Nishiguchi, N. Hirota, *Bull. Chem. Soc. Jpn.* 64 (1991) 1205-1212.
- [45] Q. -X. Liu, Z. -X. Zhao, X. -J. Zhao, Z. -Q. Yao, S. -J. Li, X. -G. Wang, *Cryst. Growth Des.* 11 (2011) 4933-4942.
- [46] M. A. Spackman, P. G. Byrom, *Chem. Phys. Lett.* 267 (1997) 215-220.
- [47] K. Ghosh, K. Harms, A. Bauzá, A. Frontera, Shouvik Chattopadhyay, *CrystEngComm.* 20 (2018) 7281-7292.

[48] P. Bhowmik, A. Bhattacharyya, K. Harms, S. Sproules, S. Chattopadhyay, *Polyhedron* 85 (2015) 221-231.

[49] T. Basak, K. Ghosh, S. Chattopadhyay, *Polyhedron* 146 (2018) 81-92.

[50] N. Sarkar, M. G. B. Drew, K. Harms, A. Bauzá, A. Frontera, S. Chattopadhyay, *CrystEngComm*. 20 (2018) 1077-1086.

[51] K. Ghosh, K. Harms, S. Chattopadhyay, *ChemistrySelect* 2 (2017) 8207-8220.

[52] K. Ghosh, K. Harms, A. Bauzá, A. Frontera, S. Chattopadhyay, *Dalton Trans.* 47 (2018) 331-347.

Table 1: Selected bond angles ($^{\circ}$) of the synthesized complex.

O(11A)-Co(1)-N(19A)	91.1(3)
O(11A)-Co(1)-N(23A)	87.6(3)
O(11A)-Co(1)-O(11A) ^a	(180)
O(11A)-Co(1)-N(19A) ^a	88.9(3)
O(11A)-Co(1)-N(23A) ^a	92.4(3)
N(19A)-Co(1)-N(23A)	85.9(3)
O(11A) ^a -Co(1)-N(19A)	88.9(3)
N(19A)-Co(1)-N(19A) ^a	(180)
N(19A)-Co(1)-N(23A) ^a	94.1(3)
O(11A) ^a -Co(1)-N(23A)	92.4(3)

N(19A) ^a -Co(1)-N(23A)	94.1(3)
N(23A)-Co(1)-N(23A) ^a	(180)
O(11A) ^a -Co(1)-N(19A) ^a	91.1(3)
O(11A) ^a -Co(1)-N(23A) ^a	87.6(3)
N(19A) ^a -Co(1)-N(23A) ^a	85.9(3)
N(2)-Co(3)-N(3)	105.0(9)
O(1W)-Co(3)-N(3)	110.0(9)
O(1W)-Co(3)-N(1)	107.0(10)
O(1W)-Co(3)-N(2)	109.9(9)
N(1)-Co(3)-N(2)	117.1(8)
N(1)-Co(3)-N(3)	107.8(10)

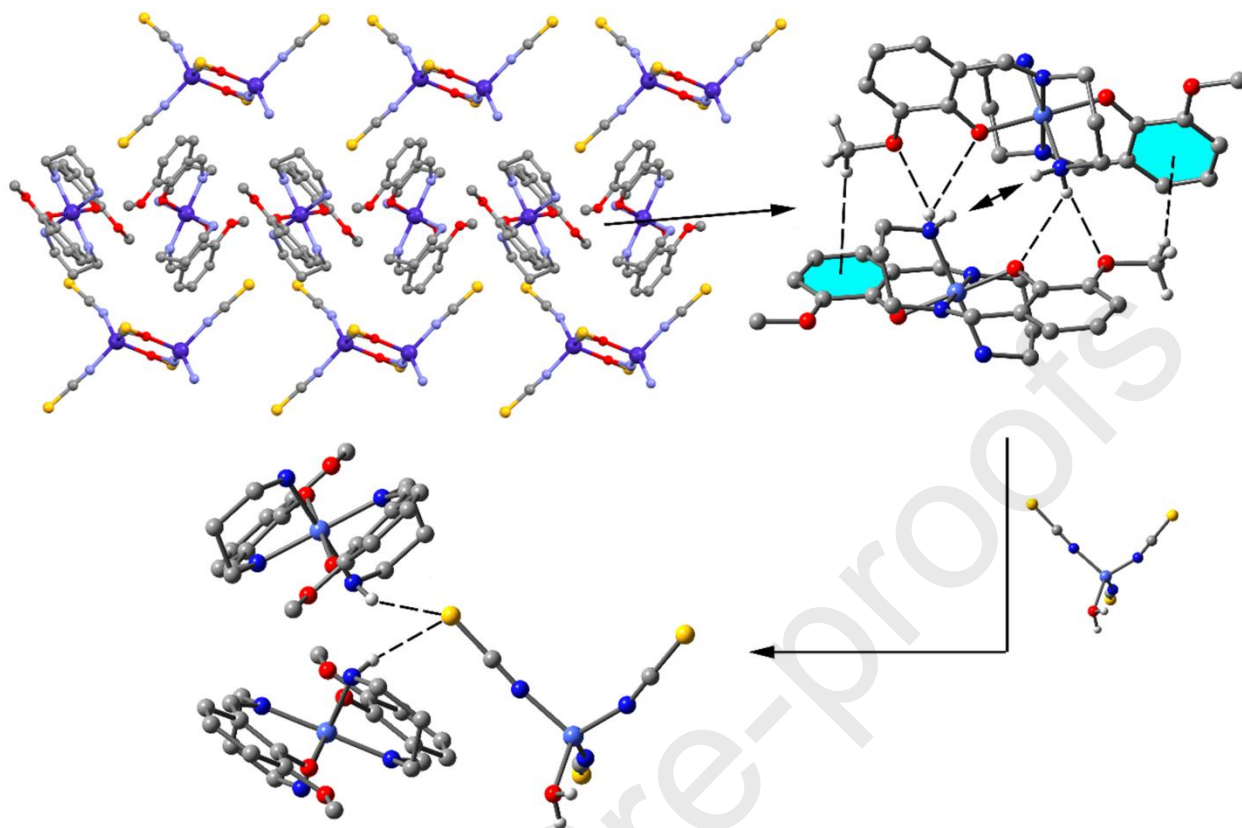
Symmetry transformation; ^a = -x,-y,-z.

Graphical Abstract (Pictogram)

A combined experimental and theoretical study on an ionic cobalt(III/II) complex with a Schiff base ligand

Kousik Ghosh, Tamal Dutta, Michael G.B. Drew, Antonio Frontera and Shouvik

Chattopadhyay



Graphical Abstract (Synopsis)

**A combined experimental and theoretical study on an ionic
cobalt(III/II) complex with a Schiff base ligand**

**Kousik Ghosh, Tamal Dutta, Michael G.B. Drew, Antonio Frontera and Shouvik
Chattopadhyay**

An ionic cobalt(III/II) complex has been synthesized and characterized by several analytical techniques. To understand the main reason behind the stabilization of this ionic cobalt(III/II)

complex, DFT calculations have been performed in detail. DFT calculations indicate that a combination of strong $\text{CH}_3 \cdots \pi$ and H-bonding interactions play a crucial role in the stabilization of this complex.

Author contribution section

Kousik Ghosh is the Principal Investigator. He synthesized the complex and characterized it by spectral and elemental analysis and performed all necessary works.

Tamal Dutta is the assistant to the Principal Investigator.

Michael G.B. Drew collected the X-ray data of the synthesized complex.

Antonio Frontera performed the theoretical study on the supramolecular interactions of the synthesized complexes.

Shouvik Chattopadhyay: The Ph.D. supervisor of Kousik Ghosh. He is also the corresponding author.